

## Supporting Information

### Heterojunction Engineering of All-Inorganic CsPbI<sub>3</sub> Perovskite for Room-Temperature High-Responsivity SWIR Photodetectors

Sydney Schmidt<sup>1#</sup>, Haley Fisher<sup>1#</sup>, Xia Li<sup>1</sup>, Jesse B. Brown<sup>1</sup>, Yuqin Qian<sup>1</sup>, Van Malmquist<sup>1</sup>, Avetik Harutyunyan<sup>2</sup>, Gugang Chen<sup>2\*</sup>, Yi Rao<sup>1\*</sup>

<sup>1</sup> Department of Chemistry and Biochemistry, Utah State University, Logan, UT, 84322, United States

<sup>2</sup> Honda Research Institute, USA, Inc., San Jose, CA 95134, United States

#### Table of Contents

**S1. Preparation of CsPbI<sub>3</sub> Perovskite Photodetector on FTO Glass.**

**S2. XRD measurements**

**S3. Absorption of CsPbI<sub>3</sub> device**

**S4. Calculation of Responsivity**

**S5. Calculation of light intensity**

**S6. Calculation of EQE**

**S7. Calculation of Gain**

**S8. Dark Current Measurements**

**S9. Determination of Specific Detectivity,  $D^*$**

**S10. 2D plot of TA measurements**

**S11. Stability Measurements**

## S1. Preparation of CsPbI<sub>3</sub> Perovskite Photodetector on FTO Glass.

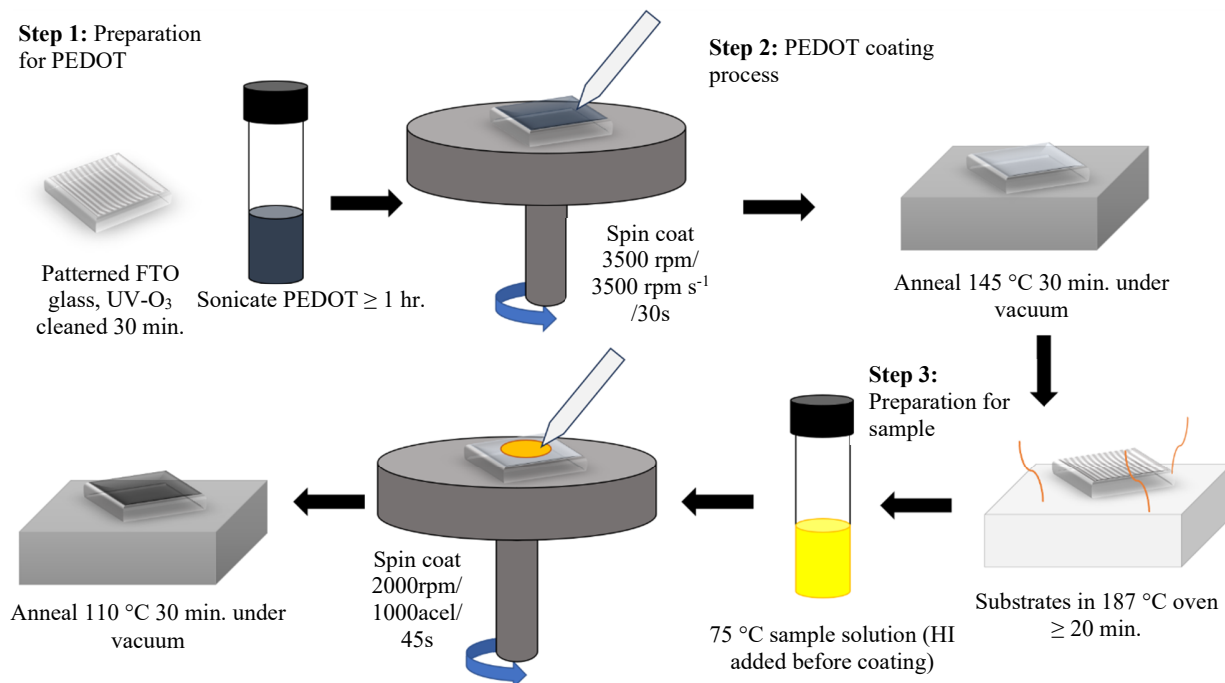


**Figure S1.** Schematic of CsPbI<sub>3</sub> device coating process. The main steps are preparation for PEDOT coating, PEDOT coating process, preparation for sample, and the sample coating process.

The CsPbI<sub>3</sub> SWIR-absorptive material was prepared using a solution of 0.5 M PbI<sub>2</sub>, with 2:1 (CsI+HAI):PbI<sub>2</sub> and HAI/(CsI+HAI)= 15% in DMF, DMSO, and GBL with the addition of 40 μL of HI per mL of sample solution added 5 minutes before coating.

## S2. XRD Measurements

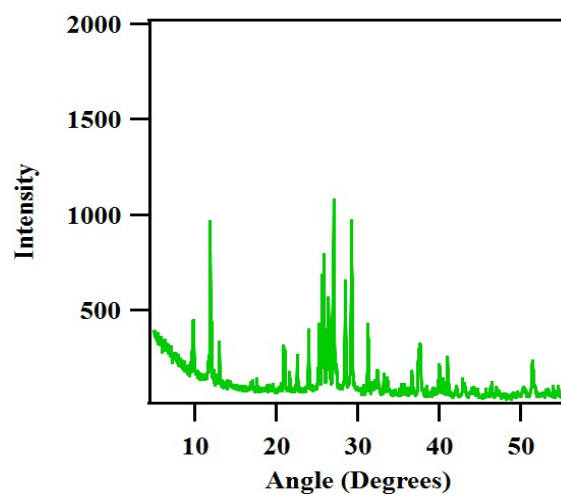


**Figure S2.** XRD spectrum of CsPbI<sub>3</sub> material with HAI and 40  $\mu$ L HI/mL.

### S3. Absorption of CsPbI<sub>3</sub> device

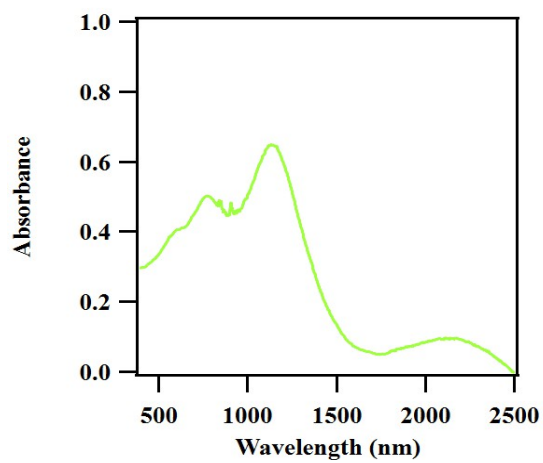


**Figure S3.** Absorption spectrum of prepared CsPbI<sub>3</sub> device.



#### S4. Calculation of Responsivity

The following example shows how the maximum responsivity measured under 0.02 mW output light power and -5 V was calculated:

$$R = \frac{I_p - I_d}{A * P} = \frac{0.001119A - 0.000886A}{0.0005 \text{ cm}^2 * (\frac{0.02 \times 10^{-3}W}{0.070686 \text{ cm}^2})} = \frac{2.33 \times 10^{-4}A}{1.4147 \times 10^{-7}W} = 1.65 \times 10^3 A/W$$

where  $I_p$  is the photocurrent (A),  $I_d$  is the dark current (A),  $A$  is the cell area ( $\text{cm}^2$ ), and  $P$  is the incident light fluence ( $\text{W cm}^{-2}$ ).

**S5. Calculation of light intensity**

$$\text{Light Intensity} = \frac{\text{Incident laser power (mW)}}{\text{Spot size of laser (cm}^2\text{)}} = \frac{\text{Incident laser power (mW)}}{0.070686 \text{ cm}^2}$$

The laser spot diameter was 0.30 cm.

### S6. Calculation of EQE

The determination of EQE provides critical insights into the performance of the photodetector, describing the ratio of generated charge carriers to incoming photons. The following example fills in the values of each parameter, using 1310 nm incident light.

$$EQE = \frac{R * hc}{e\lambda} = \frac{R(6.63 \times 10^{-34} J s)(3.0 \times 10^8 m/s)}{(1.69 \times 10^{-19} A s)(1310 \times 10^{-9} m)} = 0.90R$$

When  $R = 1.65 \times 10^3$  A/W under a bias of -5 V with 0.283 mW/cm<sup>2</sup>, the EQE is  $1.48 \times 10^3$ .

$$EQE = \frac{R * hc}{e\lambda} = \frac{R(6.63 \times 10^{-34} J s)(3.0 \times 10^8 m/s)}{(1.69 \times 10^{-19} A s)(1310 \times 10^{-9} m)} = 0.90R$$

When  $R = 1.01 \times 10^2$  A/W under a bias of -1 V with 0.283 mW/cm<sup>2</sup>, the EQE is 90.70.

## S7. Calculation of Gain

To illustrate the calculation of gain, we will use results produced by the device under different biases. The calculation below shows the simplification of known values in the gain equation, leaving the photocurrent  $I_{ph}$  as a variable. The  $I$ - $V$  data under  $0.283 \text{ mW/cm}^2$  fluence is used as the highest responsivity was achieved at this condition.  $I_{ph}$  is defined as the difference between the light-on and light-off current of cell.  $I_{ph}$  is plotted against voltage in Figure S7. The photocurrent values at different biases from -5 V to -1 V are displayed in Table S2 along with their corresponding gain. The calculation of theoretical photoconductive gain under different conditions allows the performance of the photodetector to be analyzed for varied potential applications.

$$G = \frac{I_p h\nu}{qPA} = \frac{(I_p)(6.63 \times 10^{-34} \text{ J s}) \left(3.0 \times \frac{10^8 \text{ m}}{\text{s}}\right)}{(1.69 \times 10^{-19} \text{ A s}) \left(2.83 \times \frac{10^{-4} \text{ J}}{\text{cm}^2 \cdot \text{s}}\right) (50 \times 10^{-4} \text{ cm})(0.1 \text{ cm})(1310 \times 10^{-9} \text{ m})}$$

$$G = I_p (6.09 \times 10^6 \text{ A}^{-1})$$

**Table S1.** Photocurrent under  $0.283 \text{ mW/cm}^2$  illumination and corresponding gain separated by bias.

Bias (V)	$I_{ph}$ (A)	Gain (unitless)
-5	$2.31 \times 10^{-4}$	1425.0
-4	$1.45 \times 10^{-4}$	884.2
-3	$7.48 \times 10^{-5}$	455.6
-2	$3.38 \times 10^{-5}$	205.7
-1	$1.43 \times 10^{-5}$	87.1

### S8. Dark Current Measurements

The dark current of device cells were measured inside the dehumidified shielding box at room temperature under biases from -10 mV to -5 V. Figure S4(A) shows the dark current under -1 V, and S4(B) shows the dark current under -5 V.

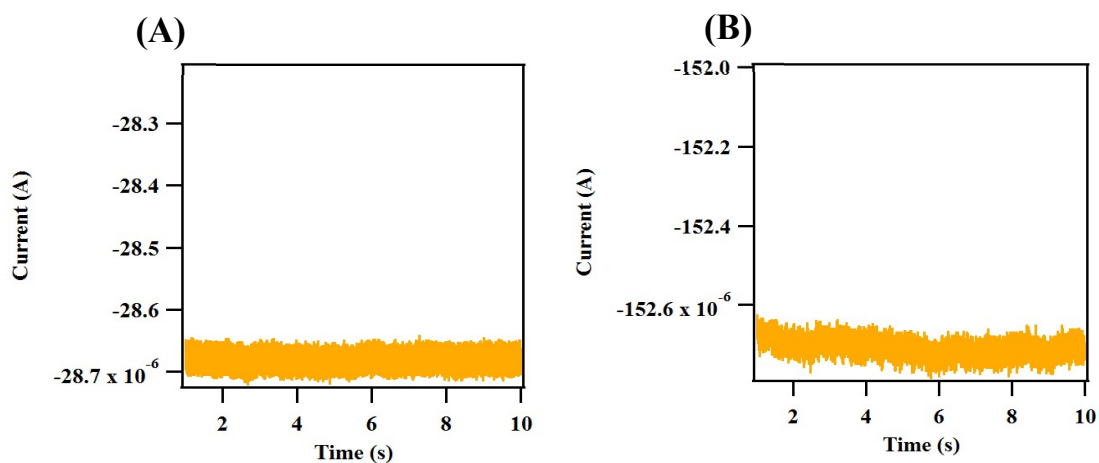


**Figure S4.** Dark current at room temperature under a bias of -1 V (A) and -5 V (B).

### S9. DDetermination of Specific Detectivity, $D^*$

To determine the NEP of this device, noise currents were gauged at varied frequencies using time-dependent dark current measurements at a bias of -5 V.

$$D^* = \frac{\sqrt{A\Delta f R}}{i_n} = \frac{\sqrt{0.1 * 0.005 \text{ cm}^2 * 500 \text{ Hz} * 1650 \text{ A/W}}}{5.50 \times 10^{-8} \text{ A}} = 9.09 \times 10^9 \text{ Jones}$$

$$i_n^2 = \frac{4\Delta N^2 \tau}{1 + 4\pi^2 f^2 \tau^2} = \frac{4qI_p G \Delta f}{1 + 4\pi^2 f^2 \tau^2}$$

Where  $q$  is the elementary charge,  $I_p$  is the net photocurrent,  $G$  is the gain,  $\Delta f$  is the bandwidth (assumed to be 1 Hz),  $f$  is the frequency at which photocurrent was measured (assuming 100 Hz) and  $\tau$  is the carrier lifetime in seconds. With lifetime on the scale of nanoseconds, the term  $4\pi^2 f^2 \tau^2$  becomes approximately zero. As such, we calculate the detectivity under at -5 V bias as follows:

$$i_n^2 = 4qI_p G \Delta f = 2.135 \times 10^{-19} \text{ A}^2$$

$$i_n = 4.621 \times 10^{-10} \text{ A}$$

$$D^* = \frac{\sqrt{0.0005 \text{ cm}^2 (1\text{Hz}) (1650 \frac{\text{A}}{\text{W}})}}{4.621 \times 10^{-10} \text{ A}} = 7.984 \times 10^{10} \text{ Jones}$$

**Table S2.** Specific detectivity at various bias if we assume  $1 + 4\pi^2 f^2 \tau^2 = 1$ .

Bias (V)	Responsivity under 0.283mW/cm <sup>2</sup> (A/W)	Specific Detectivity (Jones)
-5	1650	$7.984 \times 10^{10}$
-4	1030	$8.032 \times 10^{10}$
-3	529	$8.005 \times 10^{10}$
-2	239	$8.012 \times 10^{10}$
-1	101	$7.997 \times 10^{10}$

## S10. 2D Plot of TA Measurements

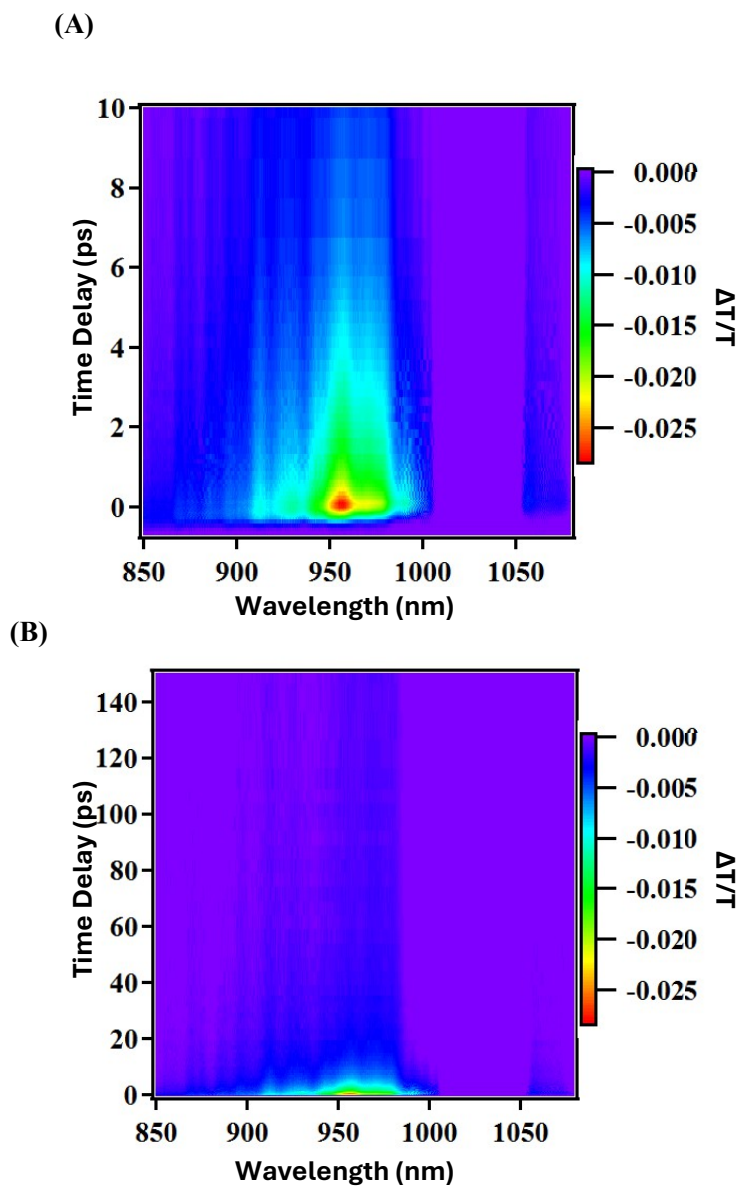


**Figure S5.** 2D plot of transient absorption spectra of the CsPbI<sub>3</sub> device with a time window of 10 ps (A) and 150 ps (B).

### S11. Stability Measurements

The stability of the device was measured over 6 days, using responsivity as the measure of performance. The maximum responsivity has been normalized in Figure S6. On day 6 since coating, the responsivity was 12% of its first-day result. The devices were stored in dry conditions.

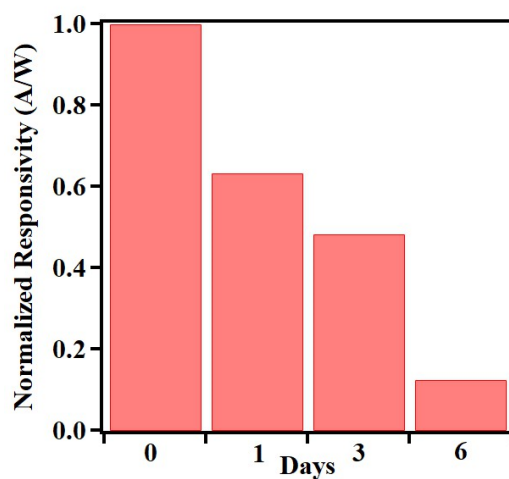


Figure S6. Normalized responsivity of the device over several days.